An averaging procedure for discharge measurement in low frequency, high amplitude fluctuations

Thomas Staubli and Alexandre Voser

Abstract

Acoustic discharge measurements (ADM) were performed in the tail water channel of the hydroelectric plant "Etzelwerk" in Switzerland. The 7 Pelton turbines installed in this plant are fed by two parallel penstocks and each of these machines is equipped with two Venturis for discharge measurement. Goal of the performed measurements was the calibration of the installed Venturi meters and of the safety devices in the penstock.

An 8 path acoustic flow meter was installed in the tail water channel, close to its exit into the lake of Zürich, 600 m downstream from the power plant. During the measurement, waves were travelling up- and downstream in the tail water channel with a period of about 7 minutes. These waves arose from the varying load conditions which had to be adjusted for the individual measuring points and induced low frequency, high amplitude oscillations of discharge at the measuring section.

By employing a non-linear identification procedure based on a least square fit, which uses the Levenberg-Marquardt algorithm, the time mean discharge Q_{ADM} could be determined with good accuracy. It is proposed that this procedure may be generally employed for cases where variations (low frequency fluctuations) occur which are beyond the limits acceptable according the IEC code.

1. Etzel power plant

The Etzel power plant was recently (1997) upgraded in order to suit the extremely varying power requirements of the Swiss railroad company (SBB). The generators of the plant were refurbished and the surge tank was completely redesigned. The power plant is equipped with 7 Pelton turbines and 3 multistage pumps, all with vertical axis. 6 of the Pelton turbines are two-nozzle turbines with 16 MW power, the largest turbine is a 6 nozzle turbine with a rated power of 44 MW. The three multi-stage pumps (14 MW, 18 MW, and 22 MW) are coupled to the turbines No 3, 4, and 7.

Plant data:

Maximum gross head   483 m
Rated discharge (turbines)   6x4m^3/s and 1x10.5 m^3/s
Length of the headrace tunnel L_{HR}=2900m
Length of the penstock L_{PS}=2500m
Length of the tail water channel L_{TW}=600m

After recommissioning the plant operator decided to recalibrate the installed discharge measurement devices in order to enable a water management optimization. These devices consist of Venturi meters which are situated immediately upstream from each of the spherical valves in the power house. There were two Venturis per turbine being equally fed from the two parallel penstocks. Furthermore, there are Pitot tubes installed at each end of the penstock with the purpose of monitoring pipe bursting. These Pitot tubes were also calibrated during the campaign and give the overall volume flux passing through each of the penstocks for all operating turbines.

With seven turbines and two pumps to be measured there were a total of 20 devices to be calibrated and it was agreed that about 80 points should be measured during this calibration campaign. Since the interruption of the normal plant operation had to be minimized, only 15 minutes between each measuring point was allowed for adjustment of a new operating point and for damping of oscillations. The smallest discharge to be measured was 0.8 m^3/s and the largest 18 m^3/s.

2. Characteristic frequencies

In order to understand typical variations in power, head, or discharge, which may arise after any power regulation, some classical estimates of characteristic frequencies were made.

The frequency and period of surge tank level oscillations is estimated as:

$$f_{ST} = \frac{1}{2\pi}\sqrt{\frac{g}{L_{HR}}} \approx 0.009 Hz \qquad T_{ST} = 2\pi\sqrt{\frac{L_{HR}}{g}} \approx 108s$$

With a speed of sound of a=1400 m/s the frequency of the water hammer in the pen stock becomes:

$$f_{WH} = \frac{a}{4L_{PS}} \approx 0.14 Hz \qquad T_{WH} = \frac{4L_{PS}}{a} \approx 7.1s$$

Speed of the waves propagating in the tail water channel (no flow) is for a water depth of H_{TW} =3m:

$$a_{wave} = \sqrt{gH_{TW}} \approx 5.4m/s$$

The frequency and period of the waves travelling up- and downstream in the tail water channel becomes:

$$f_{TW} = \frac{a_{wave}}{4L_{TW}} \approx 0.0023 Hz \qquad T_{TW} = \frac{4L_{TW}}{a_{wave}} \approx 430s$$

Fluctuations in the system due to surge tank oscillations and water hammer did not affect the accuracy of the measurements since dissipation provided enough damping after a quarter of an hour of waiting time between the individual measuring points if the power between each point was varied gradually. Power variations during each run of 30 minutes duration were generally smaller than ±1%. On the other hand, the wave travelling up- and downstream in the tail water channel were only slightly damped and caused enormous discharge fluctuations in the measuring section. Examples are shown in Figure 3. Of course, these discharge fluctuations in the tail water did influence turbine operation in no way.

3. Installation of the acoustic discharge meter

The acoustic discharge measurement was installed in the tail water channel, close to its exit into the lake of Zürich, 600 m downstream of the power plant. The meter consisted of 8 acoustic paths within one single plane (see Fig. 1) since no crossflow was expected. The path angle was 42 degrees. For the mounting of the transducers the slots for the stop logs could be used reducing the protrusion of the installation. The vertical position of the transducers was chosen as displayed in Figure 2.

Simultaneously, the free surface level at the measuring section was also measured acoustically with 2 meters (Endress&Hauser, Prosonic) mounted 300 mm above the water surface. The accuracy of this measurement was better than ±0.5 mm leading to a negligible uncertainty with respect to the water depth of 3 m.

Data acquisition was done on personal computers using the RS232 communication port or A/D-converter boards by National Instruments. For processing of the data the graphical programming language LabView from the same company was employed.
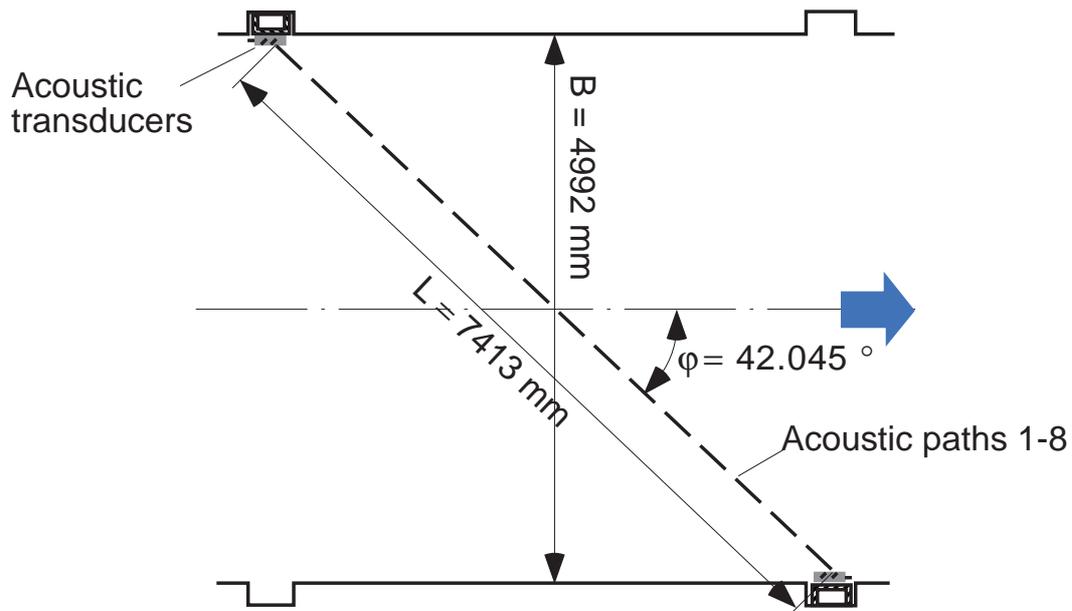
Fig. 1 Mounting of the transducers (type 7634, Accusonic) within the slots of the stop logs of the tail water channel
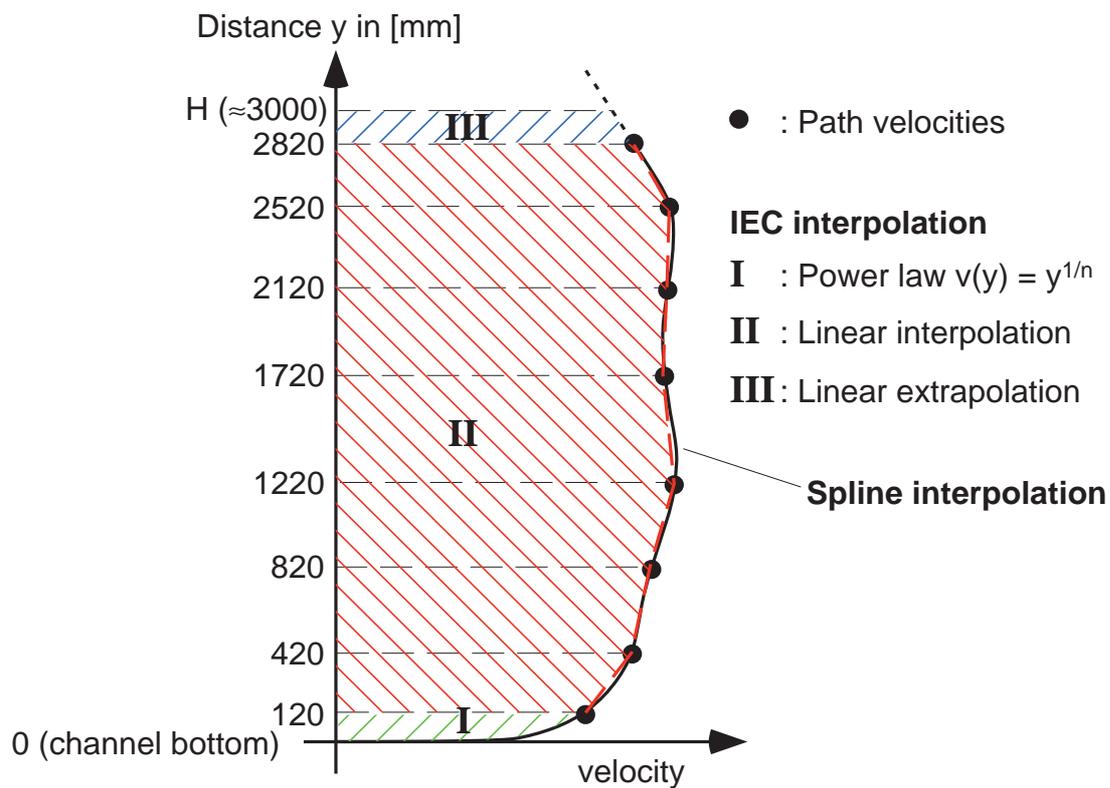

Fig. 2 Vertical transducer position in the tail water channel and interpolation procedure

4. Integration

The flow cross section was divided for integration in three zones, see Figure 2. By adding the volume fluxes of the three individual zones the total discharge could be determined.

The extrapolation formula (IEC 41) in the peripheral zone I is:

$$v(y) = v_1 (y / y_1)^{1/m}$$

where
v_1 = velocity at the distance y_1 = 120 mm from the channel bottom
m = coefficient of the exponential law being determined for each measuring point from the velocities of the two lowest paths. During the measurements it generally lay in between 5 and 6 when taking the time averaged path velocities. For the instantaneous velocity distribution extrema were found which lay in between 3 and 12.

Zone III below the free surface is the most difficult one for interpolation. The free surface velocity has to be estimated by linear extrapolation of the velocities of the two highest paths in the section. In reality the surface flow depends on the unknown air velocity in the tunnel upstream from the measuring section. Fortunately, zone III had an extension of only 180 mm which is 1/17 of the channel depth and, accordingly, uncertainties have only minor influence on the discharge integration.

The central portion with the zone II, the most important, is integrated by two different methods. On one hand, the linear interpolation in accord with IEC41 was employed. On the other, hand velocities in zone II were interpolated by a cubic spline interpolation making the distribution smooth and differentiable. Both methods led to minor differences in the results. The linear interpolation slightly underestimates discharge because it cuts off curved segments. In contrast, the spline interpolation rather gives the upper limit of possible discharge and the true value will lie somewhere in between the two data. Therefore, the final result Q_{ADM} was taken to be the linear average of the two methods.

Since data acquisition for one data set of the 8 acoustic paths took only two seconds it was possible to resolve the time-varying discharge $Q(t)$ with a resolution of about 0.2 Hz (sampling frequency = 0.5 Hz).

5. Averaging procedure

The temporal variations of discharge were dominated by the waves in the tail water channel and an averaging procedure had to be found for an accurate determination of the time mean discharge Q_{ADM}. Two typical time traces of such discharge fluctuations are displayed in Figure 3 (case A and case B). The two traces show a measurement with rather low discharge of $Q_{ADM} \cong 1.5$ m³/s. At higher discharge the relative amplitudes were smaller because of the larger damping. Difference in the time traces of the two cases lies mainly in the magnitude and phase of the third harmonic
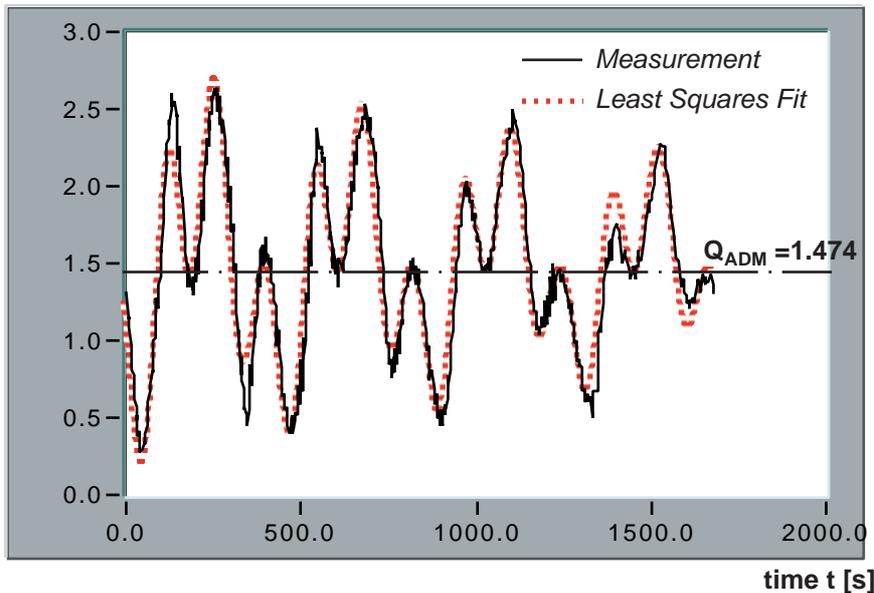
($f = 3 f_{TW}$), which showed to be the most important besides the first harmonic with frequency f_{TW}. The excitation of the higher harmonics occurred randomly depending on the instant in time when the preceding power regulation was initiated and on its magnitude and duration.

Instantaneous flow Q [m³/s]
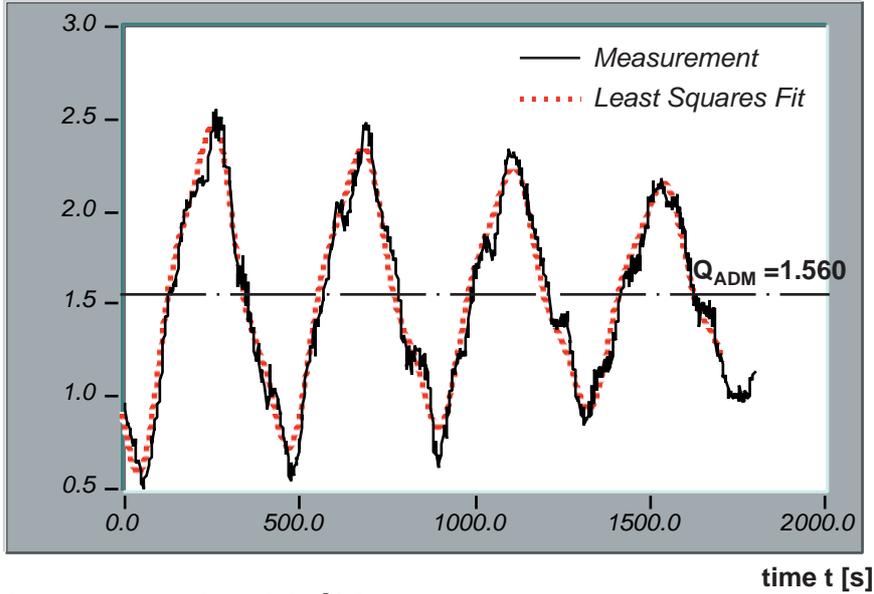
case A
$\sigma = 0.51$ m³/s
(standard deviation)

time t [s]

Instantaneous flow Q [m³/s]

case B
$\sigma = 0.47$ m³/s
(standard deviation)

time t [s]

Fig. 3 Two typical time traces of discharge fluctuations with varying phase shift of the second harmonic at $Q_{ADM} \cong 1.5$ m³/s (case A and case B).

As mentioned before, measuring of the 8 travelling times of the acoustic pulses of the 8 path acoustic meter (Accusonic 7500) lasted approximately 2 seconds. Accordingly, the sampling frequency was of the order of 0.5 Hz. However, this sampling frequency had a considerable scatter in time and, additionally, missing data points due to disturbances in the flow occurred. Therefore, in a first step of the procedure the raw data had to be interpolated to equidistant points in the time domain. This

procedure provided additionally a low pass filtering of the data in the ensemble. These interpolated data points will be referred to in the following as the individual data points $Q_{i.}$.

In a next step a least square fit was employed to identify the coefficients of a damped Fourier series (sum of trigonometric functions). This form of this function was chosen in accord with the physics of the generation and the dissipation of the oscillations in the tail water channel.

$$Q(t) = Q_{ADM} + \left(\sum_{j=1}^{k} A_j \sin(j\omega t) + B_j \cos(j\omega t) \right) e^{-\alpha t}$$

where
Q_{ADM} = time mean discharge
A_j, B_j = coefficients of the Fourier series
j = index of the identified coefficients
k = maximum number of the Fourier coefficients
α = damping coefficient
ω = $2\pi/T_{TW}$ = circular frequency of the first harmonic (identified as $\omega = 0.1468$ s^{-1} or T_{TW} = 428 s)

A maximum number of $k = 5$ harmonics in the series showed to be sufficient for an accurate determination of Q_{ADM}, the discharge being of interest.

The procedure to determine $Q_{ADM}, A_j, B_j, \alpha, \omega$ uses a Levenberg-Marquardt method that minimizes the chi-square quantity that is a least square fit (see e.g. Schwarz, 1986).

$$\chi^2 = \sum_{i=1}^{n-1} \frac{Q_i - Q_{ADM} + \left(\sum_{j=1}^{k} A_j \sin(j\omega t) + B_j \cos(j\omega t) \right) e^{-\alpha t}}{\sigma_i}$$

where
Q_i = individual data points of discharge in time
i = index of the time steps
n = maximum number of discharge data points (e.g. 800 per measurement)
χ^2 = chi-square quantity
σ_t = standard deviation of the data points (set to 1.0)

Data analysis was performed using the LabView-programming package (National Instruments, 1996) which has routines as the Levenberg-Marquardt algorithm implemented.

6. Sensitivity of the procedure on duration, location of the time segment, or on the number of identified coefficients?

The usual measurement lasted about 30 min and comprised a little more than 4 periods of the tail water oscillations.

In order to increase confidence in the chosen method we performed a series of tests of which the first concerned the variation of the identification duration.

6.1 Identification duration

Figure 4 shows the normalized results (Q_{ADM}-Q_{ref})/Q_{ref} as a function of the number of periods T_{TW} of the first harmonic of the tail water oscillation, that is the time during which the identification procedure was performed. The reference discharge Q_{ref} is taken to be the result of the identification over 4 periods T_{TW} and a number of $k = 5$ Fourier coefficients. Also displayed in Figure 4 is the arithmetic mean which is normally used as an average if no identification is employed:

$$\overline{Q} = \frac{1}{n}\sum_{i=1}^{n}Q_i.$$

The results show that the uncertainty in the determination of Q_{ADM} is reduced with increasing duration. Remarkably there is not a distinct reduction in the difference for the identified Q_{ADM} for the instances when the time window includes an integer number of periods. This means that for the identification procedure it is not a necessary condition to perform the identification over a time segment equal to an integer number of periods T_{TW}. Not so for the arithmetic mean, as expected, since the arithmetic mean yields only good results for the integer number periods.
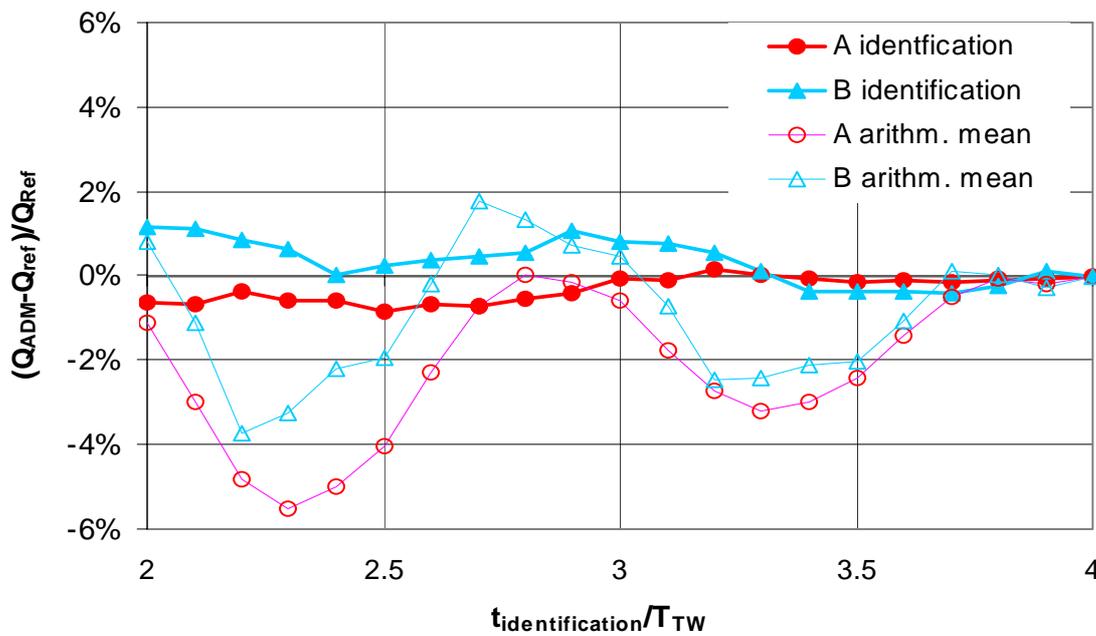

Fig 4. Evaluation of the discharge Q_{ADM} as a function of the identification duration

6.2 Selection of the location of the time segment

Figure 5 shows the normalized results $(Q_{ADM}-Q_{ref})/Q_{ref}$ as a function of the starting time t_{start} of a time segment of two periods T_{TW}. The reference discharge Q_{ref} is taken again to be the result of the identification over 4 periods and a number of $k = 5$ Fourier coefficients. The results demonstrate that identification over two periods only is definitely not enough to achieve good accuracy. Nevertheless it also can be seen that the measuring uncertainty is only little dependent upon the location of the selected time segment.

The arithmetic mean shows surprisingly good results. This is due to the fact that the arithmetic mean is performed here over exactly two periods. If not precisely averaging over two periods the arithmetic mean will yield deviations of several percent.
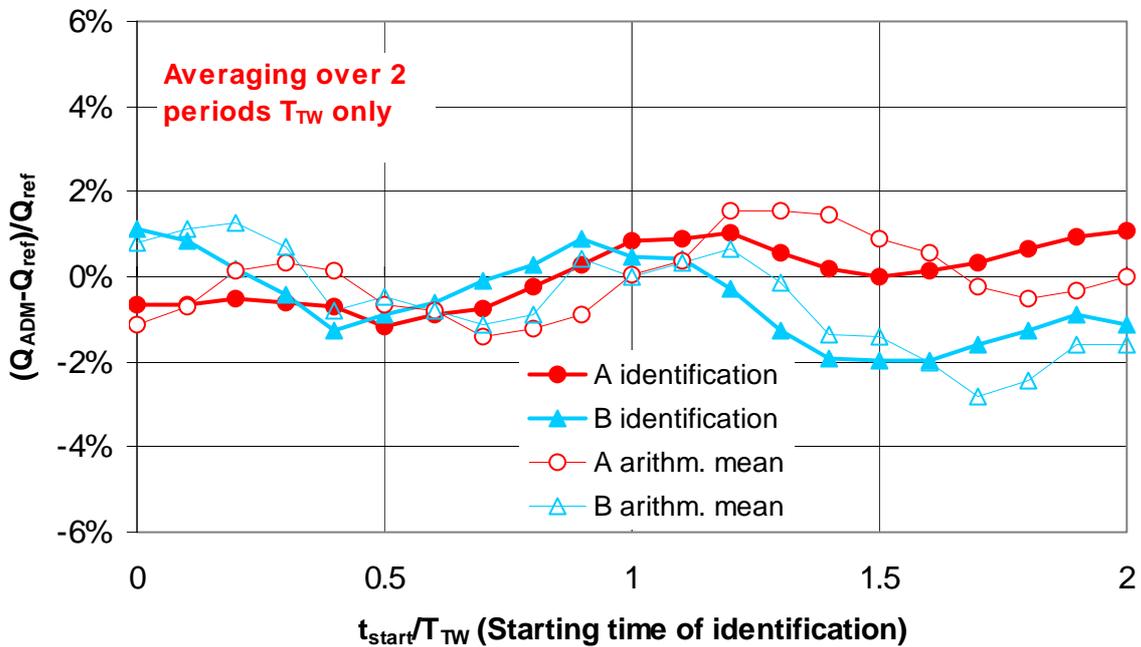

Fig 5. Evaluation of the discharge Q_{ADM} as a function of the selected time segment ($k = 5$; $t_{identification} = 856\ s = 2T_{TW}$; $T_{TW} = 428\ s$)

6.3 Influence of the number of Fourier coefficients

The only coefficient of interest resulting from the identification procedure is the mean value Q_{ADM}. All other coefficients just serve to show the good agreement of the measured data and the least-square-fit in Figure 3. However, neglecting the higher order coefficients has its impact on the mean value Q_{ADM} as shown in Figure 6. This influence disappears to a negligible quantity for number of $k > 3$.
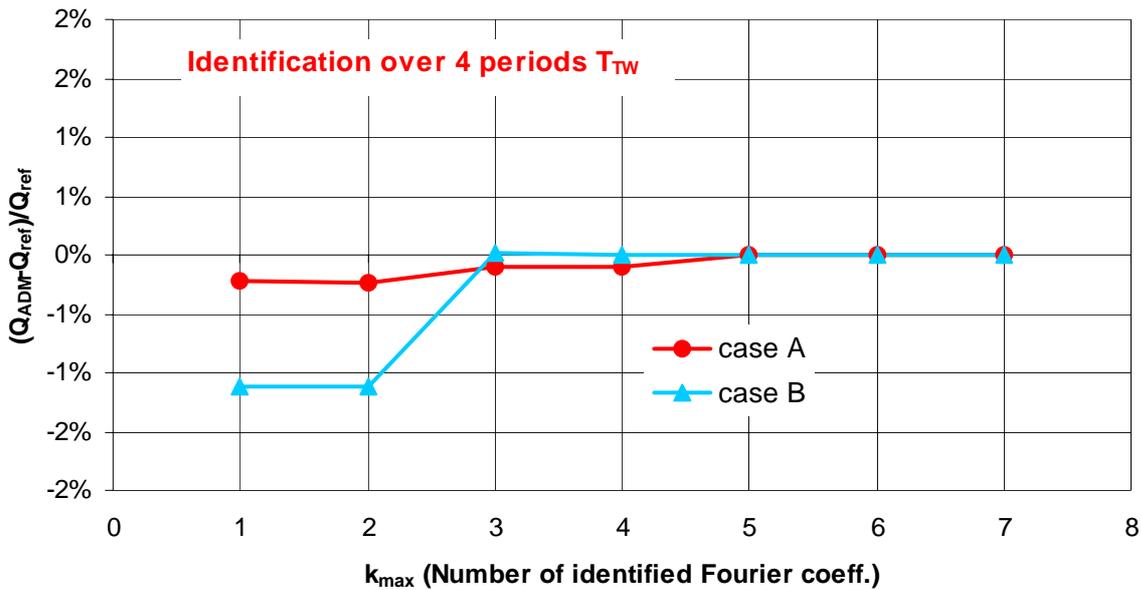
Fig 6. Influence of the number of Fourier coefficients m on the time mean discharge Q_{ADM}

7. Error analysis

Detailed analysis of the errors contributing to the overall uncertainty of the acoustic discharge measurements was performed and it could be shown that the overall uncertainty will - in spite of the high amplitude fluctuations - not exceed ±1.3 %. The errors taken into account in the analysis lay in measurement errors of the channel geometry, in the free surface measurement, in an integration error, and in an error associated with the identification procedure.

7.1 Geometry

Control measurements of the walls and the bottom of the channel confirmed a very proficient manufacturing of the channel. Variations of width and depth never exceeded 10 mm. If we assume a measuring uncertainty of $e_{geom} = \pm10$ mm in width and path length of the 8 acoustic paths then a relative uncertainty of all geometrical influences on discharge is calculated to be:

$$f_{geom} = \pm0.3\%.$$

7.2 Water level measurement

The free surface level at the measuring section was measured acoustically with 2 separate meters mounted approximately 300 mm above the water surface. In the time mean no variation of the surface was observed within the measuring section, and long scale gravity waves as well as short surface scale waves did not influence the time averaged result. According to the data sheet of the transducers accuracy is 0.1 % of full scale. With a full scale range of 500 mm this leads to an uncertainty of

$e_{surface} = \pm 0.5$ mm. The measuring error during tests is negligible with respect to the calibration error to the reference of the channel depth. This calibration was performed before the tests for quiescent surface conditions. The accuracy of this calibration was better than ±5 mm leading to uncertainty of the depth measurement of

$$f_{depth} = \pm 0.2\%.$$

7.3 Integration error

The closest upstream disturbance in the tail water channel was a 30 degree bend situated about 100 m upstream and it was assumed that this disturbance does not induce any cross flow within the measuring section. Furthermore, protrusion effects of the acoustic transducers were corrected on the bases of numerical calculation of the disturbed flow field in the proximity of the transducers (Voser, 1996). This correction procedure resulted in path velocities which were reduced by 0.3% with respect to the measured ones.

The integration error is divided into three individual errors according to the three zones of integration (Fig. 2):

Zone I: In general, the exponent m of the law of the wall during the measurements lay in between 5 and 6 when taking the time average path velocities. The measuring uncertainty in this zone may be estimated by calculation discharge with the extreme values of $m = 3$ and $m = 12$ found in the instantaneous velocity distributions. The difference in the total discharge calculated for these two values amounted to ±0.4% of the mean discharge Q_{ADM}. The error estimate based on the extreme values of m will be on the safe side:

$$f_{zoneI} = \pm 0.4\%.$$

Zone II: The measuring uncertainty in this zone may be estimated by calculation discharge with two different integration methods using a linear or a spline interpolation of the data in between the 8 path velocities. The difference between the two integration methods was 0.4 % of Q_{ADM} resulting in an estimate of the uncertainty of

$$f_{zoneII} = \pm 0.2\%.$$

Zone III: Due to the important uncertainty in estimating the free surface velocity (wind effects etc.) it was estimated that the error may reach up to 10 % of the discharge in zone III. However, since this zone contributes only about 5 % to the total discharge, the relative error with respect to Q_{ADM} becomes small:

$$f_{zoneIII} = \pm 0.5\%.$$

In spite of the systematic nature of these errors they are combined according IEC193 (1965) to a global uncertainty in the discharge integration by the root-sum-square method:

$$f_{integ} = \pm\sqrt{f^2_{zoneI} + f^2_{zoneII} + f^2_{zoneIII}} \cong \pm 0.7\%.$$

7.4 Identification error

Since the function described with the damped Fourier series is only an approximation of the time traces and since there is little experience with the errors arising from the identification procedure the uncertainty of the identification was estimated to be $f_{ident} = \pm 0.5$ %. When considering the variations of Q_{ADM} in the Figures 4, 5, 6, this estimate is on the safe side and will include all other effects which have not been taken into account in this error analysis.

7.5 Total measuring uncertainty

Combining the component uncertainties by the root-sum-square method, the relative total uncertainty is obtained:

$$f_{ADM} = \pm\sqrt{f^2_{integ} + f^2_{geom} + f^2_{surface} + f^2_{ident}}$$

$$f_{ADM} = \pm\sqrt{0.007^2 + 0.002^2 + 0.003^2 + 0.01} \cong \pm 1.3\%.$$

This result means that the total measuring uncertainty is as low as it could be expected for a "good" current-meter measurement and steady-state conditions. The code IEC41 gives as an estimate for current-meter measurement uncertainty in an open channel with rectangular cross section:

$$f_{CM} = \pm 1.2\% \quad to \quad 2\%.$$

8. Conclusion

In spite of the enormous fluctuations of discharge in the tail water channel it was possible to measure the time mean discharge Q_{ADM} with good accuracy. A series of tests provided good confidence in the applied method basing on a non-linear identification procedure to determine Q_{ADM}. The overall measuring uncertainty was estimated to be $e_{ADM} < \pm 1.3\%$, which is a quite good value for an open channel measurement.

The IEC code (IEC41: 1991) demands steady state conditions, i.e. the variation of power should not exceed ±1.3% and the variations of specific hydraulic energy shall not exceed ±1 % of the average value. However, it may be assumed that low frequency, harmonic variations, which are beyond the acceptable limits, quite often occur in hydroelectric plant measurements, especially if long waiting times are not ac-

ceptable. Such low frequency variations can be approximated by a damped Fourier series and it is proposed that the procedure employed in this paper, using a non-linear identification based on a least-square-procedure, may be generally used to improve the measuring accuracy.

Acknowledgement

References

International Standard CEI/IEC-41, Field Acceptance Tests to Determine the Hydraulic Performance of Hydraulic Turbines, Storage Pumps and Pump-Turbines, 1991

International Standard CEI/IEC-193, Hydraulic Turbines, Storage Pumps and Pump-Turbines Hydraulic Performance - Model Acceptance Tests, 1965

National Instruments Corporation, LabView - Manuals, 1996

Schwarz, H.R., "Numerische Mathematik", Teubner, 1986

Voser, A., CFD-Calculations of the Protrusion Effect and Impact on the Acoustic Discharge Measurement Accuracy, IGHEM-Seminar, Montreal, 1996